RESEARCH ARTICLE   OPEN ACCESS

A Design of H-Bridge Converter for Power Conversion System

Mr. C.Sudhakar, Mr.C.Pavan Kumar, Mr.Y.Damodharam
Kuppam Engineering College, Dept. of EEE

ABSTRACT

Now a day's wind turbine power outputs are 2MW and above. If transmission of high power with low voltage conversion system will suffer from a high transmission current. The transmission of high current from wind generator to grid we require larger cable size which is increases losses and cost of the cables as well as voltage drop. This paper proposes a modular, medium voltage and high- power converter topology for the large permanent magnet wind generator system, eliminating the grid-side step-up transformer. The converter modules are cascaded to achieve medium voltage output. Each converter module is fed by a pair of generator coils with 90° phase shift to get the stable dc-link power. The power factor correction (PFC) circuit enables the generator to achieve unity power factor operation and the generator armature inductance is used as ac -side PFC boost inductance. At the grid-side, H-bridge inverters are connected in series to generate multilevel medium voltage output and the voltage-oriented vector control scheme is adopted to regulate the converter active and reactive power transferred to the grid. The Simulation results with a 2MW wind turbine system. The proposed system can successfully deliver power from the wind generator to the grid.

Index Terms —Cascaded H-bridge converter, high- power medium voltage converter, permanent magnet generator, trans-former-less, wind power.

I. INTRODUCTION

TODAY, a doubly fed induction generator (DFIG) with a partially rated rotor-side converter is the mainstream technology in the market for large wind turbines. Meanwhile, a permanent magnet generator (PMG) interfaced to the grid through a full power converter is increasingly being adopted due to its higher power density, better controllability, and reliability, especially so during grid faults [1]. The voltage level of a wind power converter is usually in the range of 380 V-690 V due to generator voltage rating and voltage limitation of power electronics devices. Therefore, the power converter is connected to the grid via a step-up transformer to match the grid voltage level (10.5V~35KV) in the wind farm collection system. In the low voltage (690 V) system, when wind turbine power is larger than 500 kVA, several power converters are connected in parallel to handle the increasing current [2]–[6]. The large current transfer also results in a parallel connection of multiple cables and causes substantial losses (I^2R), voltage drop as well as high cost of cables and connections. This disadvantage can be avoided by placing the step-up transformer into the nacelle. However, the bulky and heavy transformer significantly increases the mechanical stress of the tower. Instead of paralleling converters and cables, another alternative to transfer high power is to use medium voltage transmission, where the current is reduced and the step-up transformer may not be needed if the converter output voltage level can reach the grid voltage (10.5kV~35 kV) [2], [3]. Hence, a transformer-less, medium voltage high power converter system would be an attractive technology for large wind

turbines, especially when today's wind turbine power rating is approaching 5MW and above [4]–[6]. Since the system current rating can be a good indicator for the cable and connection cost and losses, Table I shows the current rating comparison of a 5MW system with different voltage levels. As can be seen, the increase of voltage level to 10 or 35 kV can significantly reduce the current ratings.

TABLE I
WIND TURBINE CURRENT RATINGFOR
DIFFERENT VOLTAGE LEVELS

S.No	WIND TURBINE POWER(MW)	VOLTAGE(KV)	CURRENT(A)
1	5.0	0.69	4400
		10	303
		35	86

Medium-voltage high-power converters have been widely used for motor drive applications, such as neutral point clamped (NPC) converters and cascaded H-bridge converters, which benefit from multilevel voltage output, less voltage stress, and better harmonic spectrums [7]. The cascaded H-bridge converter is recognized as more suitable for industrial product in the sense of modular structure, high reliability, and fault-tolerant ability. In addition, it is the only available and practical multilevel converter topology that may meet the voltage level of more than 10 kV subject to the voltage rating of power electronic devices. For motor drive applications, the cascaded H-bridge

converter needs several independent power sources for the inputs, which are usually provided by an input trans-former with multiple secondary windings [8]. Whereas, in a wind power conversion system, the multiple generator coils can be used as the independent sources for the converter modules.

Based on this, this paper presents a modular permanent magnet wind generator and medium-voltage converter system, aiming to reduce the system current rating by cascading converter modules as shown in Fig. 1(a). Each module is composed of a rectifier fed from isolated generator coils, a dc-link, and an H-bridge inverter, as shown in Fig. 1(b).Unlike the conventional cascaded H -bridge converter used in motor drive applications, the wind power converter serves as the interface between the wind generator and the grid. At the generator side, each converter module requires a stable voltage source input, where a pair of generator coils with 90º phase shift are connected either in parallel or in series to reduce the low frequency power ripple. This will require a special winding arrangement of the generator as well as a control strategy for the generator-side rectifier. A single- switch boost-type power factor correction (PFC) circuit is used as the rectifier, enabling the generator unity power factor operation and also maintaining the converter cell dc - link voltage under different wind speeds. At the grid side, the cascaded H-bridge converter is facing the grid instead of the motor. Then, the control scheme should allow active power and reactive power transferred to the grid as well as dealing with different grid conditions such as grid faults. The voltage oriented vector-control strategy is used to achieve independent control of active power and reactive power fed into the grid and phase - shifted PWM is used for modulating the cascaded converter. The proposed topology and control method is verified by a 2MW, 11kV grid simulation system and also by a 3kW experimental system.

Fig. 1. Configuration of the proposed system. (a) Electrical configuration of the wind generator and multilevel high-power converter system; (b) topology of the converter cell.

II. CONVERTER TOPOLOGY AND CONTROL METHOD

The modular wind power converter system is shown in Fig. 1. As seen, in each phase, several low voltage rating modules (converter cells) are connected in series to achieve medium voltage output (10.5~33KV). Therefore, the converter can be directly connected to the grid via the filter inductance, eliminating the step -up transformer. Each converter cell is composed of an ac-tive rectifier, a dc - link, and an H-bridge inverter, as shown in Fig. 1(b). In fact, the active rectifier can take different structures such as full- bridge, half-bridge, bridgeless converter or single- switch PFC [14]. Since the generator only requires unity power factor operation and the power flow is unidirectional (from generator to the grid), the single-switch type PFC can meet the requirement with the simplest structure and is adopted as in Fig. 1(b). This circuit has only one active switch that needs to be controlled, which simplifies the control complexity, especially when the number of converter modules is significant. The system neutral point O is grounded via some impedance to improve the system phase to ground fault tolerance and blocking the zero-sequence current [15]. During normal operation, the voltage across the grounding impedance will be a small portion of the system common-mode (CM) voltage as a result of switching. While during phase to ground fault, the phase voltage will be seen on the impendence, which can be used to detect the ground fault condition.

A .Converter Cell Topology and Design Considerations

In Fig. 1(b), each isolated generator coil is rectified through a PFC circuit to achieve unity power factor operation and maintain the dc-link voltage of the converter cell under different wind speeds. In addition to the dc component, the output power of a single -phase PFC circuit contains an ac component ($2w_g$) with twice the generator stator frequency, as shown in (1)

$$P_{g\_single}(t) = e_g \cdot i_g = E_m \sin(\omega_g t) \cdot I_m \sin(\omega_g t)$$
$$= \frac{E_m I_m}{2} - \frac{E_m I_m}{2} \cos(2\omega_g t) \qquad (1)$$

Where E_m and I_m are the amplitudes of the generator coil back-EMF (e) and current (i) respectively. w_g is the generator stator frequency. This power pulsation with the frequency of $2w_g$ will cause dc- link voltage ripple and affect the H-bridge inverter output. For direct- drive PMG, since the stator frequency w_g is relatively low (usually below 15 Hz), it requires a large dc-link capacitor to reduce the voltage ripple, which significantly increases the system cost. The capacitor lifetime will affect system reliability as well. In this paper, the output of two generator coils with 90º phase shift
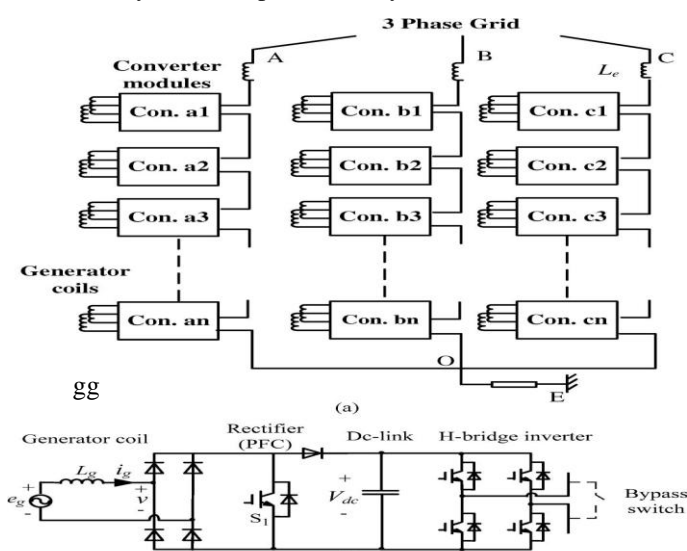
are rectified and connected either in parallel or in series to cancel out the ac power component, as indicated

$$P_{g\_pair}(t) = E_m \sin(\omega_g t) I_m \sin(\omega_g t)$$
$$+ E_m \sin\left(\omega_g t + \frac{\pi}{2}\right) \sqrt{2} I_m \sin\left(\omega_g t + \frac{\pi}{2}\right)$$
$$= E_m I_m. \qquad (2)$$

The ac component of the dc-link power is thus eliminated and the power keeps constant. Accordingly, the converter cell topology will transform from Fig. 1(b) to be as in Fig.2.

In Fig. 2(a), the two generator coils of 90° phase shift and their PFC circuits are connected in parallel. Therefore, the power from the generator side is constant as shown in (2) and the size of the dc-link capacitor can be reduced.

The dc-link capacitor only needs to handle the power ripple from the H-bridge inverter and the high-frequency switching harmonics. Another alternative is to connect the two generator coils in series as shown in Fig. 2(b); this structure can also meet the constant power condition and the dc-link voltage will be twice of the parallel structure as in Fig. 2(a). Correspondingly, the module grid-side inverter can adopt a three- level NPC-type converter to match the dc-link voltage level if the power electronics device of the same voltage rating is used for both rectifier and inverter.

An advantage of the structure in Fig. 2(b) is that the dc-link voltage is doubled. Therefore, the grid voltage level can be reached with half the number of modules cascaded compared with the structure in Fig. 2(a), and hence the total number of the independent generator coils required is reduced, which is useful considering the limited number of generator coils and the complexity of winding terminal connection in practice. It should also be noted that, since the neutral point [point O in Fig. 2(b)] in NPC inverter is actively clamped by the front generator-side rectifier.

The intrinsic neutral point voltage balancing problem in NPC converter is not a concern here. However, in the series structure, although the whole dc-link power from the generator is constant, the neutral point O still has low frequency ripple (2w) due to (1), which may affect the NPC bridge voltage output to some extent. Since the control strategies for the two types of converter cells in Fig. 2 are similar, this paper will focus on the design and control of the parallel structure in Fig. 2(a).
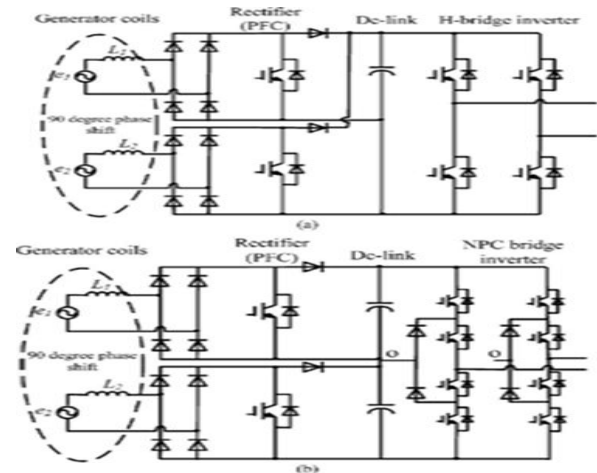
Fig.2. Converter modules with two generator coils of 90^0 phase shift connected in parallel or in series and the corresponding rectifier and inverter topology. (a) Parallel rectifier and a H-bridge inverter. (b) Series rectifier and an NPC inverter.
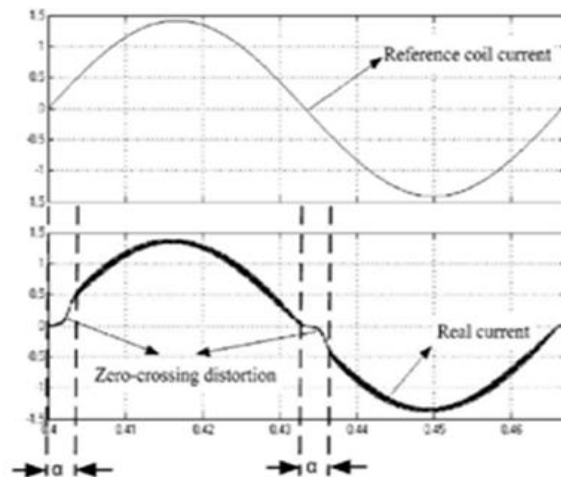
Fig. 3. Reference current and real current (current ripple and zero-crossing distortion).

In the proposed topology, generator armature inductance is used as ac-side boost inductance, as shown in Fig. 2 (L_1 and $L2$), without requiring extra inductance. The design value of generator armature inductance is mainly determined by the PMG stator current ripple constraint and the current zero -crossing distortion. As observed in Fig. 3, although the coil current reference is sinusoidal, the real coil current will have current ripple and current zero -crossing distortion. The current zero-crossing distortion is an intrinsic problem associated with the single-switch boost-type PFC circuit, since the polarity of the rectifier voltage [v in Fig. 1(b)] is determined by the coil current direction (which two diodes conduct) [16]. In theory, larger inductance will reduce the current ripple while causing larger current zero-crossing distortion.

The lower limit of generator inductance is then given by the amplitude of the current ripple δI_m as well as the dc-link voltage V_{dc} and the switching

frequency f_s [17], as follows:

$$L_g \geq \frac{V_{dc}}{4\delta I_m f_s} \qquad (3)$$

Where I_m is the peak value of the generator coil sinusoidal cur-rent, and δ is the factor to determine the allowable current ripple. From (3), smaller current ripple requires larger inductance. On the other hand, the inductance value will affect current zero-crossing distortion. The current distortion angle at zero-crossing can be calculated by [17]

$$\alpha = 2arctg\left(\frac{\omega_g L_g I_m}{E_m}\right) \qquad (4)$$

Where E_m is the peak value of the generator back-EMF. From (4), the larger the inductance is, the larger the zero-crossing distortion angle will be, which affects the current waveform and reduces the generator power factor. Therefore, the upper limit of the inductance should meet

$$L_g \leq \frac{E_m}{\omega_g I_m} tg \frac{\alpha_{cr}}{2} \qquad (5)$$

Where α_{cr} is the maximum allowable current distortion angle. Hence, the design value of generator inductance should meet (3) and (5) as well as other generator specifications, such as generators short-circuit current.

B.Model Of Generator-Side Rectifier And Control Strategy

The generator- side rectifier model can be derived from the basic structure in Fig. 1(b), regardless of whether the rectifier is based on the parallel or series structure as shown in Fig. 2. The relationship between coil current, generator back-EMF, and rectifier ac-side voltage (v) is given by

$$e_g = v + L_g \frac{di_g}{dt} \qquad (6)$$

Where e is the generator coil back-EMF, v is the rectifier ac-side voltage, current and L are the coil current and inductance, respectively. From (6), it can be seen that the coil current i can be controlled by applying appropriate converter voltage, as shown in the simplified circuit diagram in Fig. 4(a). In order to reduce the generator losses, the generator is controlled to be operated under unity power factor. In this case, the coil current is in phase with the generator back-EMF and the phase diagram is shown in Fig. 4(b).
Meanwhile, the rectifier ac-side voltage v is determined by the duty cycle of the main switch (S_1), dc -link voltage, and the coil current direction, which is expressed as follows:

$$v = (1-d)V_{dc}sign(i_g) \qquad (7)$$

Where d the rectifier is main switch duty cycle; V_{dc} is the dc-link voltage; sign (i) represents the current direction, which will determine which two diodes conduct in the rectifier in Fig. 1(b) and the

polarity of v is then determined accordingly. Based on (6) and (7), the control strategy can be developed, where the current control loop will enable the coil current to track the generator back-EMF to achieve unity power factor operation. For the parallel or series structure in Fig. 2, the two rectifiers can be controlled independently.
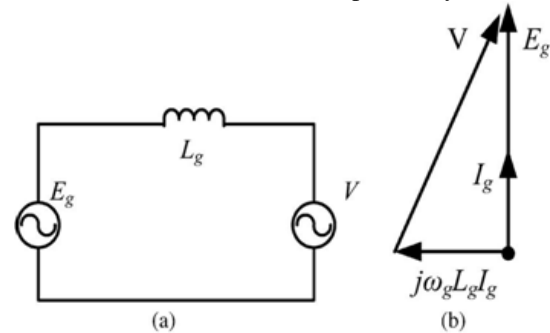
Fig. 4. Diagram of the generator side rectifier. (a) Simplified rectifier circuit diagram; (b) phasor diagram under unity power factor.

C.Rectifier Control Unit
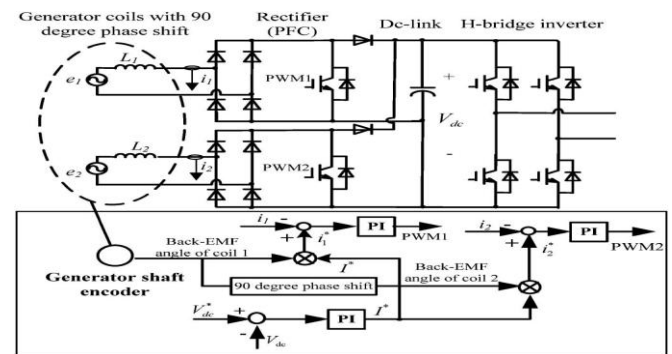
Fig.5. Rectifier control diagram.

The whole control diagram for the paralleled rectifier in Fig. 2(a) is developed as shown in Fig. 5, which has outer dc-link voltage control loop and inner current control loop. The outer loop maintains the dc- link voltage of the converter cell under different wind speeds and its output provides the reference of the current amplitude for the inner current loop. Together with the phase angle of generator back-EMF, the coil current reference can be found. The inner current loop enables the coil current to keep sinusoidal and track the generator back-EMF. Meanwhile, the current loop can also achieve proper power sharing between the two paralleled rectifiers. PI controllers are used here as the outer voltage loop controller as well as inner current loop controller and the proportional and integral gains can be determined by the required control bandwidth and based on the model in (6) and (7). Note that, as shown in the topology in Fig. 5, the generator back-EMF (e_1 and e_2) cannot be measured directly. Therefore, the phase angle of generator coil back-EMF is reconstructed based on the generator rotor position

and the distribution of stator coils (angle). The generator rotor position is measured via the shaft encoder as shown in Fig. 5. Once the rotor position is obtained, the phase angle of generator coil back-EMF can be reconstructed based on the stator coil location.

D.Vector Control Unit

At the grid-side, the H-bridge inverters of each converter cell are connected in series to achieve medium voltage multi-level output, interfacing with the grid via the filter inductance as shown in Fig. 1(a). If assuming the dc-link voltage of each series connected converter cell are the same (the dc-link voltage is regulated by the rectifier), then the cascaded H-bridge converter can be modeled as one voltage source converter and its output voltage is shared equally among the converter cells. Then, the grid-side cascaded H-bridge converter can be modeled in d-q frame, which rotates synchronously with the grid voltage vector, as follows [18]–[20]:

$$\begin{cases} L_e \frac{di_d}{dt} = -R_e i_d + \omega_e L_e i_q - S_d + u_d \\ L_e \frac{di_q}{dt} = -R_e i_q - \omega_e L_e i_d - S_q + u_q \end{cases} \quad (8)$$

Where L_e and R_e are the grid inductance and resistance, u_d, u_q, i_d and i_q are the grid voltages and currents in the d_q frame, respectively. S_d and S_q are the output voltages of the cascaded H-bridge converter along the d-axis and q-axis in the switching average model. w_e is the grid line frequency.

If the d-axis of the rotating frame is oriented along the grid voltage vector $(u=0)$, then the converter active power P and reactive power Q can be formulated by

$$\begin{cases} P = u_d i_d + u_q i_q = u_d i_d \\ Q = u_d i_q - u_q i_d = u_d i_q. \end{cases} \quad (9)$$

From (9), it is shown that the converter output active power and reactive power can be controlled independently by control-ling the d-axis and q- axis current. Based on this, the vector control diagram for the grid-side cascaded H-bridge converter is developed as illustrated in Fig. 6 [19], [21]. As seen, the active power and reactive power demand is given as the reference. From (9), the d- axis and q- axis current reference can be found by dividing the active power and reactive power by the grid-voltage (u_d). The active power demand P* is usually set based on the wind speed and wind turbine characteristic to achieve maximum power point tracking (MPPT). The reactive power Q* is usually generated to support the grid voltage. The current loop controller adopts the PI controller to control the d-axis and q-axis current independently. The grid voltage angle θ_e, which is used for coordinate transformation, can be derived through phase-locked loop (PLL), as described in [22].

In the above analysis, the cascaded H-bridge converter is regarded as a single voltage source converter. The modulation strategy must be developed to modulate the cascaded H-bridge converter once the voltage reference (u*$_{a,b,c}$) is obtained from the current loop, as shown in Fig. 6. The modulation of cascaded H-bridge inverter employs the so-called phase- shifted carrier PWM, where the carrier signal of each cascaded converter cell has a phase shift with each other by a certain degree and is compared with the common modulation signal. This modulation scheme can enable the converter to achieve multilevel voltage output when several converter cells are connected in series. It can also guarantee the equal power sharing between the cascaded cells, since the output voltage of each cell is the same (only has a small phase shift) and the current is the same (because they are in series). Fig. 7 illustrates the modulation scheme with three stages of H- bridge inverter cells in series. Fig. 7(a) shows the modulation signals (obtained from current loop output) for the first-stage H-bridge inverter, which are compared with the carrier signal to get gate signal of the left and right phase leg of the H-bridge cell. Note that, the two modulation signals are out of phase with each other so that the output voltages of H-bridge cell have a unipolar (three-level) output as shown in Fig. 7(b).
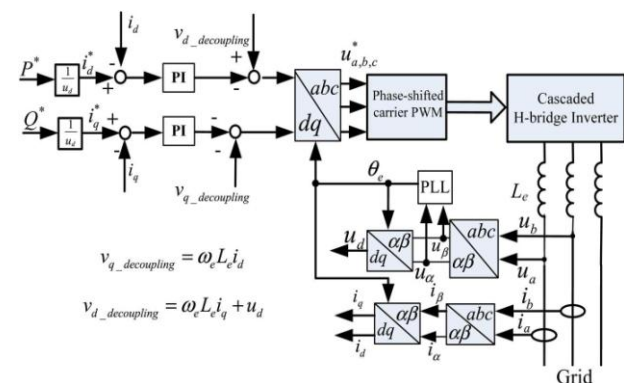
Fig. 6. Vector control diagram of the grid-side cascaded H-bridge converter.

Similarly, the other two stages are modulated with the same modulation signal as in Fig. 7(a), but with phase-shifted carrier signals as in Fig. 7(c). Subsequently, the output voltage of the cascaded H-bridge cells (three stages) has seven voltage levels, which optimizes the harmonics due to the switching. It should also be noted that, besides the dc component, the output power of each H-bridge inverter cell contains power ripple as well, and its frequency is twice of the fundament output voltage frequency (the same as grid frequency in this case). However, the power ripple frequency here is much higher than the one from the generator side. The ripple frequency is 100 Hz for a 50-Hz grid and 120 Hz for a 60-Hz grid. Therefore, it may be filtered with a relatively smaller dc-link capacitor.
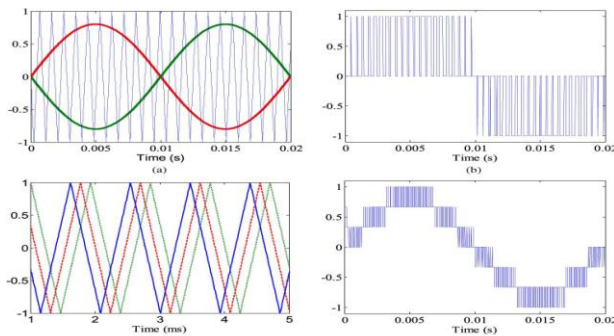
Fig. 7. Illustration of the modulation scheme of cascaded H-bridge inverter. (a) Modulation of one H-bridge inverter; (b) output voltage of one H-bridge inverter ;(c) carrier signals of three-stages H-bridge inverters; (d) output voltage of the cascaded H-bridge inverter with three stages (seven levels).

E.Generator Design Considerations

The wind generator must be designed to be compatible with the converter topology in terms of stator winding arrangement, insulation requirement, and so on. As shown in Fig. 2, every converter cell needs a pair of generator coils with $90°$ phase shift. The conventional three-phase generator may not meet this requirement. Hence, the multiphase (more than three phases) generator is used to achieve the required phase shift between different coils. Fig. 8 presents the stator winding diagram of a six-phase six-pole PMG (dual three-phase windings, $30°$ phase shift). As seen, there are a number of coils with $90°$ phase shift, depending on the number of poles of the generator, which is quite a few for direct -drive PMG. In practice, coils of the same phase (belonging to different poles) can be connected flexibly, either in series or connected out separately to meet the application needs, for example, to meet the voltage rating requirement of each cell. Note that, besides the six- phase generator, the PMGs with multiples of six phases (i.e., 12, 18, 24) will also have coil pairs with $90°$ phase shifts. The use of a multiphase generator also benefits from fault-tolerant ability and reduced torque ripple [23]. Taking the six-phase generator shown in Fig. 8 for example, the third, fifth, seventh order harmonics in the generator back-EMF will not cause the low-frequency torque ripple. The lowest order of torque ripple will be 12th order, caused by 11th and 13th harmonics interaction with the sinusoidal current.
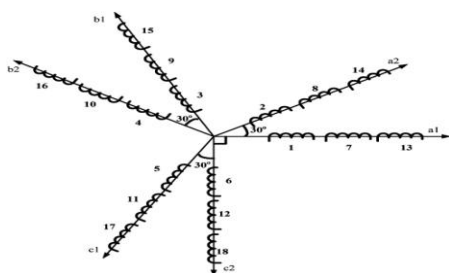
Fig. 8. Stator winding diagram of a six-phase PMG.

In the proposed topology, the generator

insulation should withstand grid voltage level (10~33 kV) due to the elimination of the step-up transformer. The insulation issues may be a challenge in the generator design. Generators which operate on these voltage levels are commonly made of form-wound coils covered with three insulation layers: strand insulation, turn insulation, and ground-wall insulation (insulation between coil and the stator core). The ground- wall insulation is imposed to the highest voltage stress at end winding terminal, which corresponds to ground voltage. Also, semiconductive coating and ripple springs are used to eliminate the possibility for external partial discharges (corona) caused by air voids between ground-wall insulation and a stator core [5].

F.System Level Operation Strategy And Fault Tolerant Discussion

The proposed converter is facing the grid; the system should also be able to handle grid faults, such as voltage dip and unbalance, which may be a challenge in the practical system. The control strategies for riding through the grid faults used in two-level full power converters might be adopted and adjusted for the proposed structure [18], [26]. For example, a dump resistor bank might be needed to handle the deep voltage drop. A PLL and advanced current controller which may track the positive sequence voltage/current might be used to manage the grid unbalance.

III. SIMULATION VERIFICATION

The simulation model for a 2MW generator and converter system and 11kV grid is built in MATLAB/Simulink to verify the proposed topology and control method. In the simulation, the PMG has 48 coils, which can form 24 pairs of coils with $90°$ phase shift. Therefore, the three-phase cascaded converter has eight stages and can output 17 voltage levels. The dc-link voltage of each converter module is set at 1400V to meet the grid voltage of 11kV. Based on the generator inductance design rules given in (3) and (5), the generator inductance is chosen to be 10mH to limit the current ripple within 10% of the maximum current and no more than $10°$ for the current zero-crossing distortion. Meanwhile, the dc-link capacitor is chosen to be $8000\mu F$ to reduce the dc- link voltage ripple (caused by H-bridge inverter power ripple) to be within 1% of the nominal dc-link voltage.The simulation results are shown in Fig. 9. Once the wind speed reaches cut-in speed and the dc-link voltage is regulated to 1400 V, the grid -side contactor will close and the cascaded H-bridge converter starts to operate and control the active and reactive power fed into the grid. Fig. 9(a) shows the converter output voltage, which has 17 voltage levels. Fig. 9(b) shows the grid phase voltages (a,b,c) the system start at t=0.03s. As seen, there is no inrush current. In addition, the converter current is controlled in phase with the grid voltage,

transferring only the active power to the grid (The positive cur-rent flow is defined as from the converter to the grid). Fig. 9(c) presents the results for converter transferring both reactive power and active power to the grid with a power factor of 0.8, which validates the vector control scheme for the grid-side converter. Fig. 9(d) shows the converter output current wave-form during wind speed increase. The current increases at t=0.5s and the system active power increases from 1.14 to 1.5 MW. As seen, the converter output current increases to maintain the active power transfer. If a larger voltage dip happens, the converter current may reach the limit and the generator-side rectifier should reduce the power output and the generator speed may increase. Fig. 9(d) shows the generator back-EMF and Fig. 9(e) shows coil current, where the generator coil current is controlled in phase with the generator back-EMF, thus achieving unity power factor to reduce the generator losses, which validates the generator control scheme.

(a)

(b)

(c)

(d)

(e)
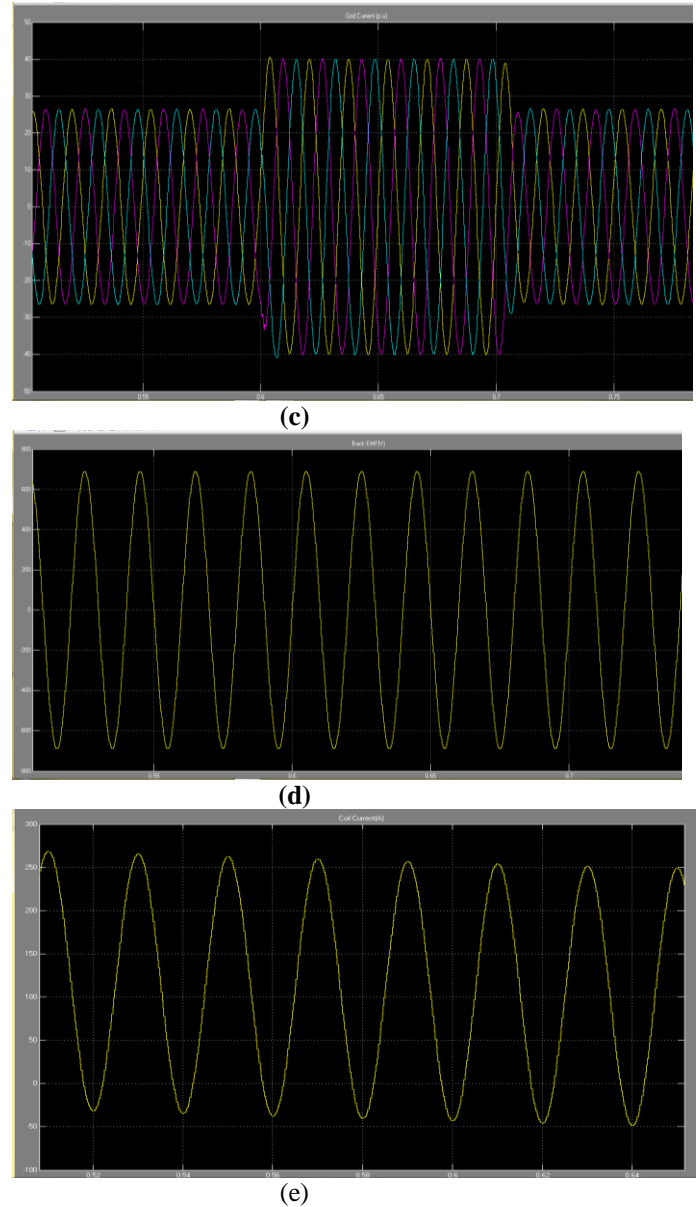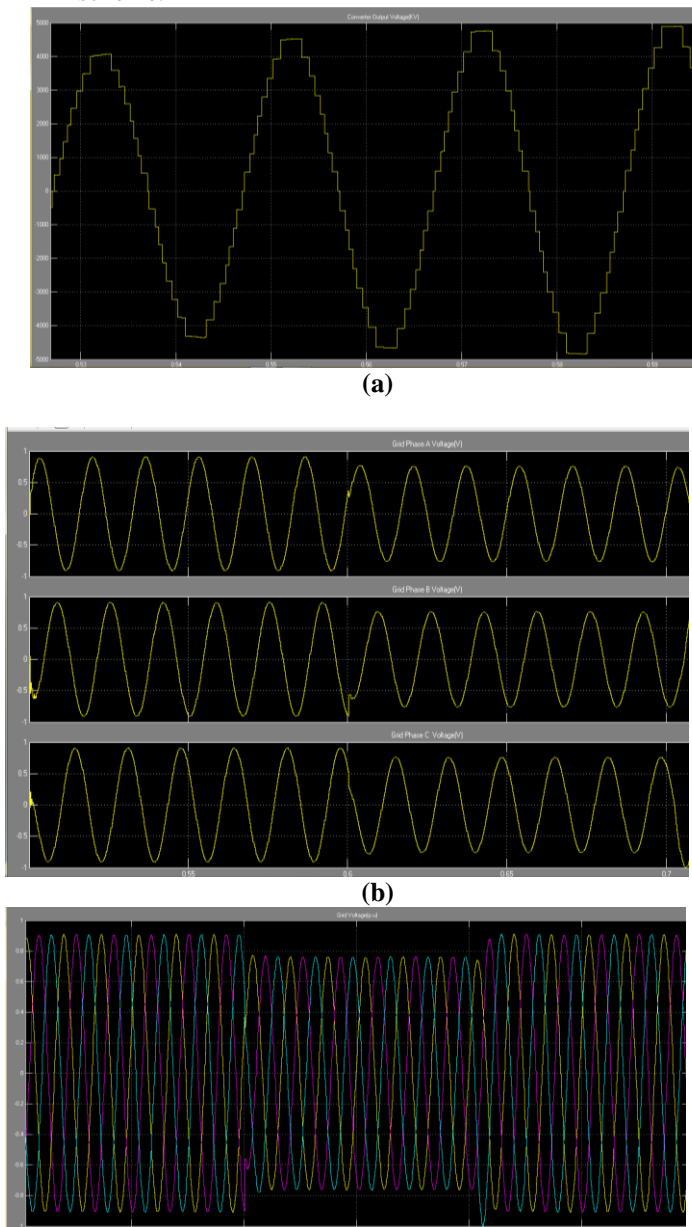
Fig. 9. Simulation results. (a) Grid-side cascaded converter output voltage (17 levels); (b) grid phase voltage (power factor is 0.8); (c) grid voltage and current during 20% voltage dip; (d) generator back-EMF; (e) coil current.

IV. CONCLUSION

The proposed system can reduce the cable losses, cost of cables and connections by reducing the current, which provides a solution for the power conversion of large wind turbines. The generator coils with 90° phase shift are connected via rectifier either in parallel or in series to achieve a constant dc- link power. The vector-controlled cascaded H-bridge converter can successfully transfer power from the generator to the grid with independent active power and reactive power control ability. The Simulation results performed with 2MW PMG, 11kV grid system.

REFERENCES
[1] C. Ng, M. Parker, and P. Tavner, "A multilevel modular converter for a large light weight wind turbine generator," *IEEE Trans. Power Elec-tron.*, vol. 23, no. 3, pp. 1062–1074, May 2008.
[2] H. Li and Z. Chen, "Design optimization and evaluation of different wind generator systems," in *Proc. IEEE ICEMS'08 Conf.*, Oct. 2008, vol. 2, pp. 2396–2401.
[3] Faulstich, J.K Stinke, and F. Wittwer, "Medium voltage converter for permanent magnet wind power generators up to 7 MW," in *Proc. EPE Conf.*, Sep. 2009, pp. 9–17.
[4] M. Sztykiel, "Overview of power converter designs feasible for high voltage transformer-less wind turbines," in *Proc. IEEE ISIE 2011 Conf.*, Jun. 2011, pp. 1420–1425.
[5] E. Spooner, P. Gordon, and C.D. French, "Lightweight, ironless-stator, PM generators for direct-drive wind turbines," in *Proc. Int. Power Electronics, Machines and Drives Conf.*, Mar. 2004, vol. 1, pp. 29–33.
[6] D. Vizireanu, X. Kestelyn, and S. Brisset, "Polyphased modular direct-drive wind turbine generator," in *Proc. EPE'05 Conf.*, Sep. 2005, vol. 1, pp. 1–9.
[7] J. M. Carrasco, L.G. Franquelo, and J.T. Bialasiewicz, "Power-elec-tronic systems for the grid integration of renewable energy sources: A survey," *IEEE Trans. Ind. Electron.*, vol. 53, no. 4, pp. 1002–1016, Aug. 2006.
[8] F. Blaabjerg, F. Iov, T. Terekes, and R. Teodorescu, "Power elec-tronics-key technology for renewable energy systems," in *Proc. Power Electronics, Drive Systems and Technologies Conf.*, Feb. 2011, pp. 445–466.
[9] Mullance, G. Lightbody, and R. Yacamini, "Wind turbine fault ride through enhancement," *IEEE Trans. Power Electron.*, vol. 20, no. 4, 1929–1937, Nov. 2005.
[10] M. Chinchilla, S. Arnaltes, and J. Burgos, "Control of perma-nent-magnet generators applied to variable speed wind energy systems connected to the grid," *IEEE Trans. Energy Convers.*, vol. 21, no. 1, 130135, Mar. 2006.

C.Sudhakar has obtained his B.Tech. (Electrical and Electronics Engineering) from JNTUA University, Anathapur in 2009. He is currently pursuing his M.Tech. (Power Electronics) from JNTU Anantapur. His research area of interest includes Power Electronics and Power Systems.

C.Pavankumar has obtained his B.Tech.(Electrical and Electronics Engineering) from JNTUA University, Anathapur in 2009. He is currently pursuing his M.Tech. (Power Electronics) from JNTU Anantapur. His research area of interest includes Power Electronics and Power Systems.

Y.Damodharam has obtained his B.Tech.(Electrical and Electronics Engineering) from JNTUH University, Anathapur in 2006. He completed M.Tech in Power systems on High Voltage Engineering from JNTU Kakinada in the year 2008. Currently working as Associate Professor in Kuppam Engineering College in the Department of EEE. His area of research is high Voltage engineering, power systems.